

Supporting Information for the article:

Reversible Assembly and Disassembly of Gold Nanorods Induced by EDTA and its application in SERS Tuning

T. S. Sreeprasad and T. Pradeep*

*DST Unit on Nanoscience, Department of Chemistry and Sophisticated Analytical Instrument Facility,
Indian Institute of Technology Madras, Chennai-600 036, India*

**For correspondence, Email: pradeep@iitm.ac.in Fax: + 91-44 2257-0545*

Figure S1: UV/Vis spectrum and TEM images of parent GNRs

Figure S2. TEM images of end-to-end assembled rod where EDTA is attached directly on GNR tips.

Figure S3. TEM images of small islands of GNRs formed at 0.2 mM EDTA.

Figure S4. UV/Vis spectra showing the spectral changes of side-by-side assembled GNRs.

Figure S5. UV/Vis spectra showing detection of Pb (II) in ppb range.

Figure S6. UV/Vis spectra showing the insignificance of anions in disassembly.

Figure S7. TEM images of GNRs after disassembly (GNRA_{AD})

Figure S8. TEM images of small assembled structures after disassembly.

Figure S9. FT-IR spectra of the assembly and disassembly.

Figure S10. TEM images of ladder-like assemblies formed at pH = 3.5.

Figure S11. TEM image of randomly arranged rods upon addition of EDTA-Pb(II) complex.

Figure S12. UV/Vis spectra as well as TEM images showing the disassembly with Fe (II) and Fe (III).

Supporting information S13. Table showing the assignment of SERS features of CV.

Figure S14. Raman spectrum of parent GNR.

Figure S15. Comparison of SERS activity of aggregated gold nanospheres and GNR assemblies.

Figure S16. Reproducibility of SERS spectra from GNR assemblies

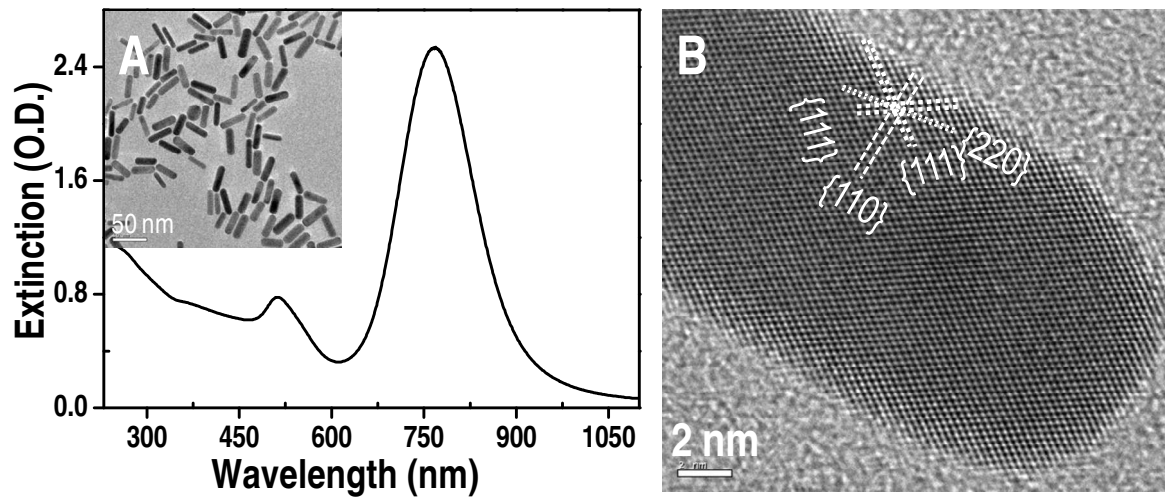


Figure S1.A) UV/Vis spectrum of GNRs showing the LSP centered at 765 nm and TSP around 511 nm corresponding an aspect ratio 3.4. Inset shows a large area TEM image of the pristine GNRs (Scale bar 50 nm). B) Lattice resolved image of the tip of a GNR showing the lattice structure depicting the defect free nature of the rod.

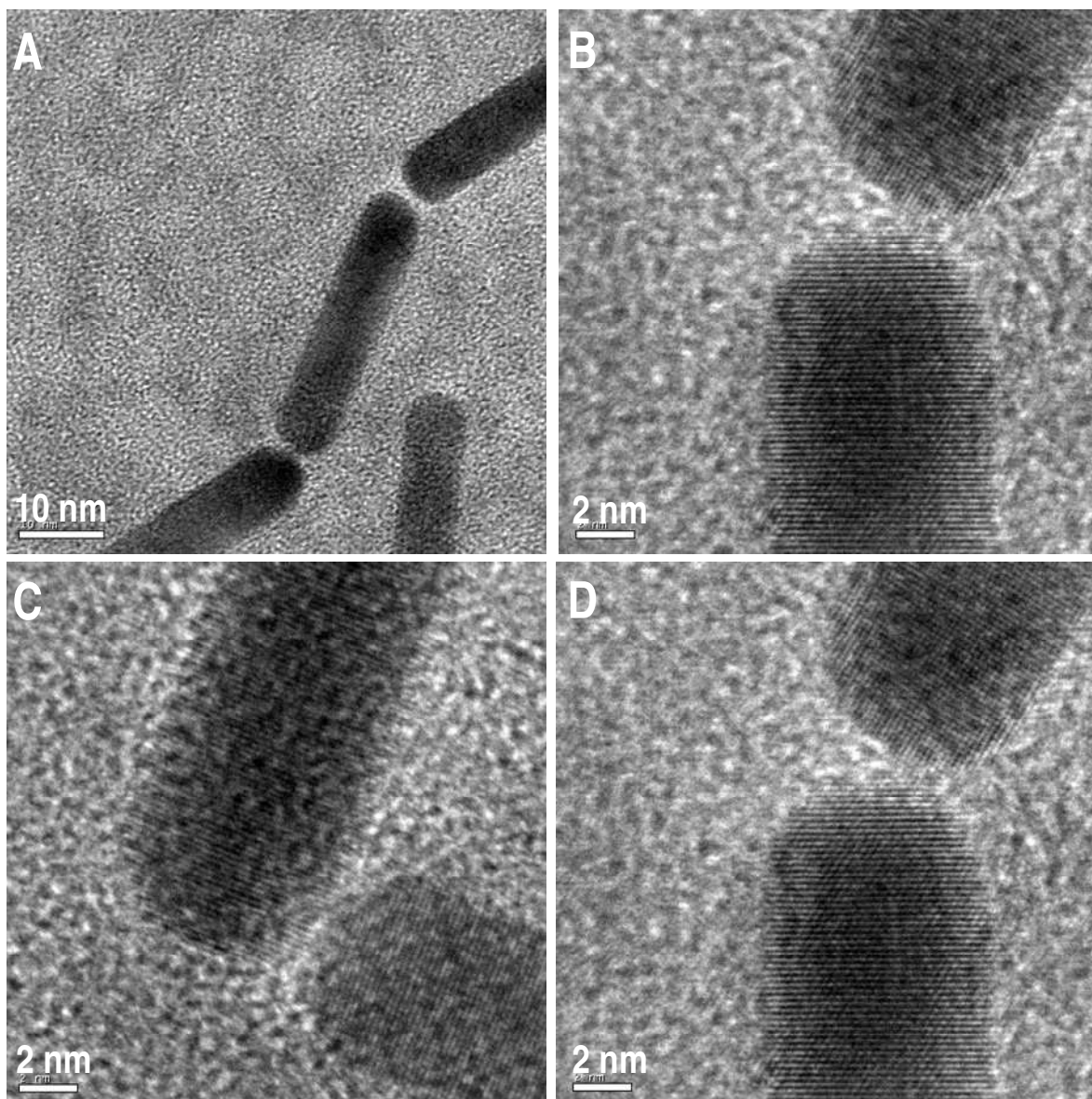


Figure S2. TEM images of end-to-end assembled GNRs where EDTA is directly attached onto the surface. Distance between the rods here is ~ 1 nm.

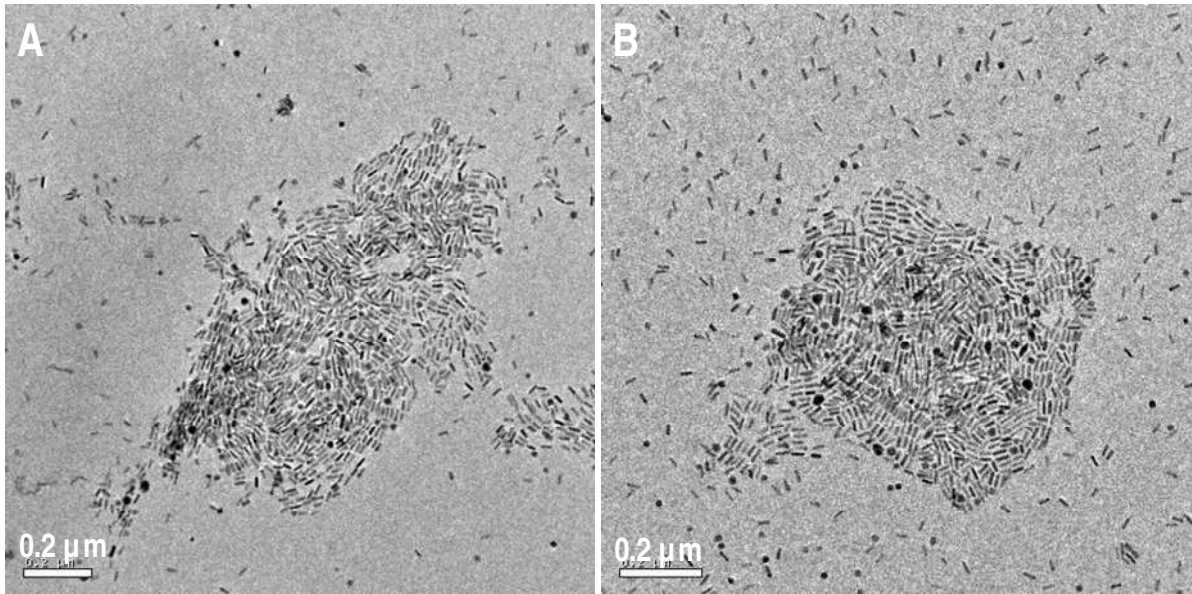


Figure S3. TEM images of small islands of GNRs with a side-by-side orientation formed at 0.2 mM concentration EDTA.

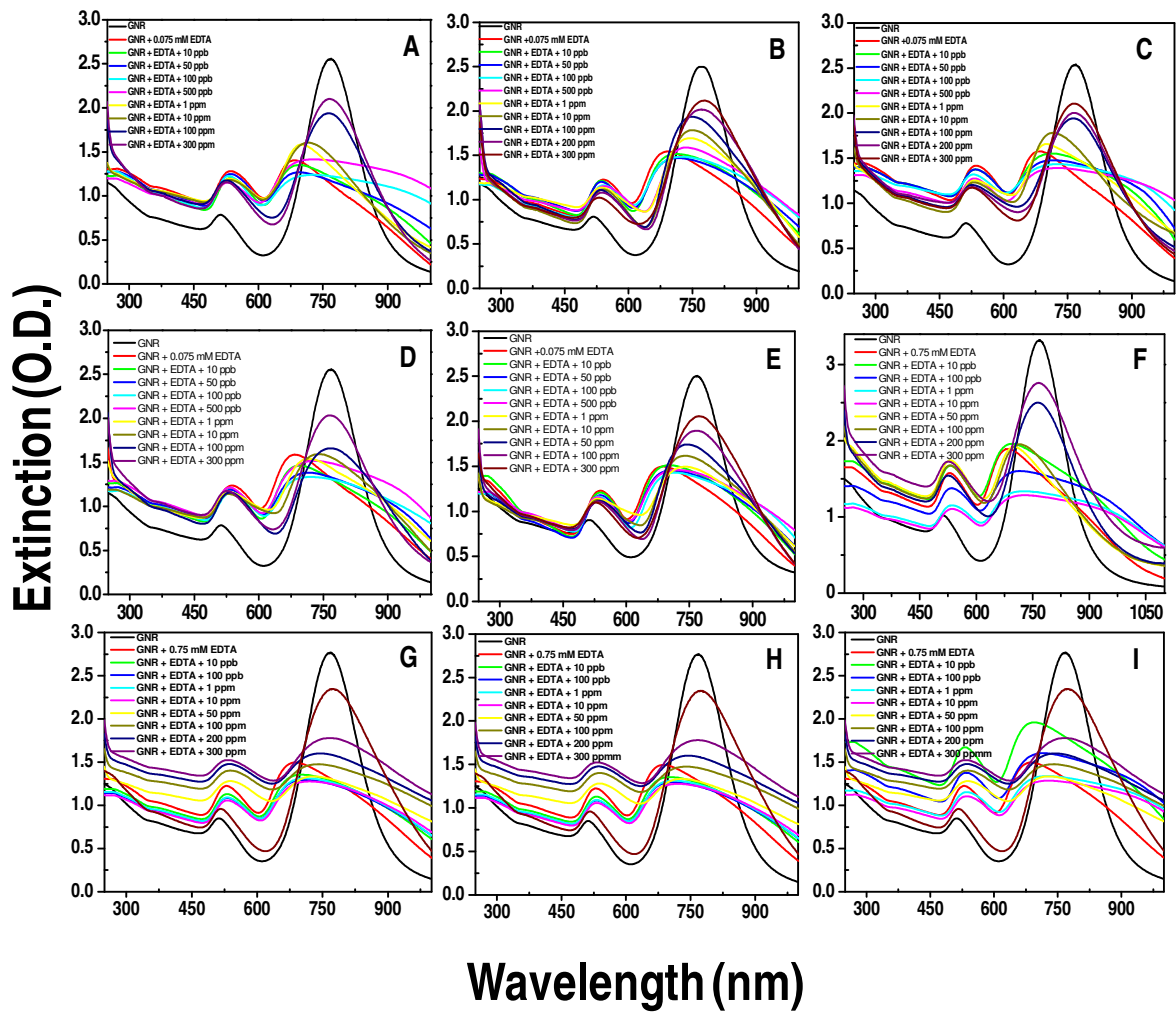


Figure S4. UV/Vis spectra showing the spectral changes happening to the side-by-side assembled GNR-EDTA (0.75 mM) sample upon addition of A) Zn(II), B) Cd(II), C) Hg(II), D) Mn(II), E) Cu(II), F) Ni(II), G) Co(II), H) Cr(II), I) Fe(II).

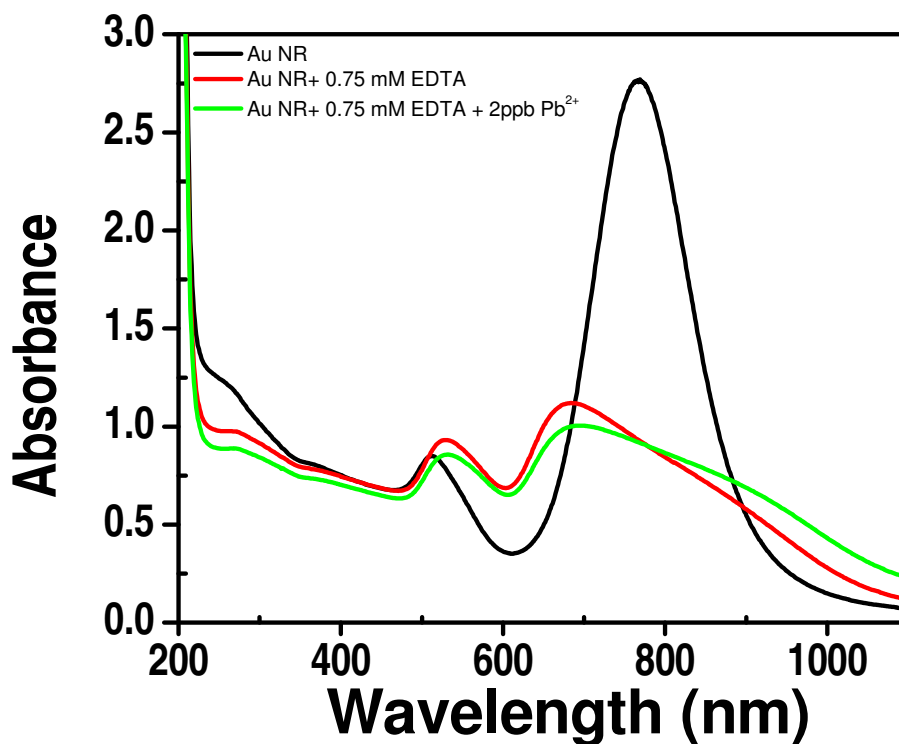


Figure S5. UV/Vis spectra showing the spectral change of side-by-side assembled GNR-EDTA (0.75 mM) sample upon addition of 2 ppb Pb(II)

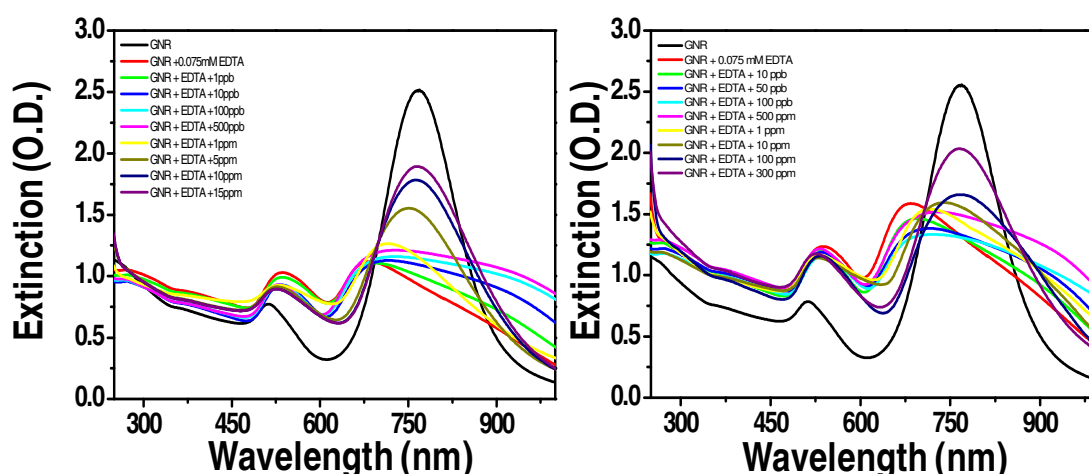


Figure S6. UV/Vis spectra showing the disassembly of side-by-side assembled GNR-EDTA (0.75 mM) sample with A) Pb(CH₃COO)₂ and B) Pb(NO₃)₂.

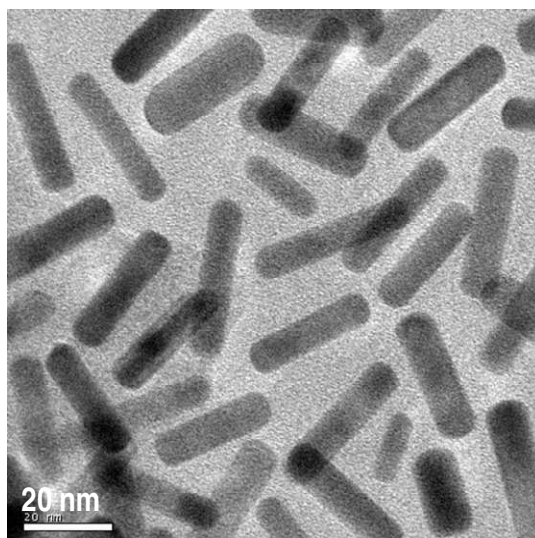


Figure S7. TEM image of GNRs after disassembly showing no preferential order

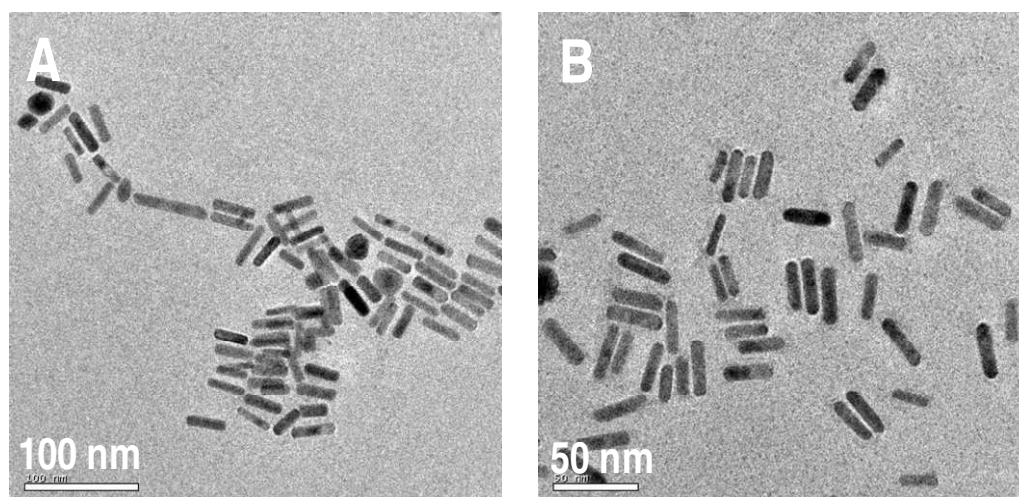


Figure S8. TEM images of small assembled structures after disassembly.

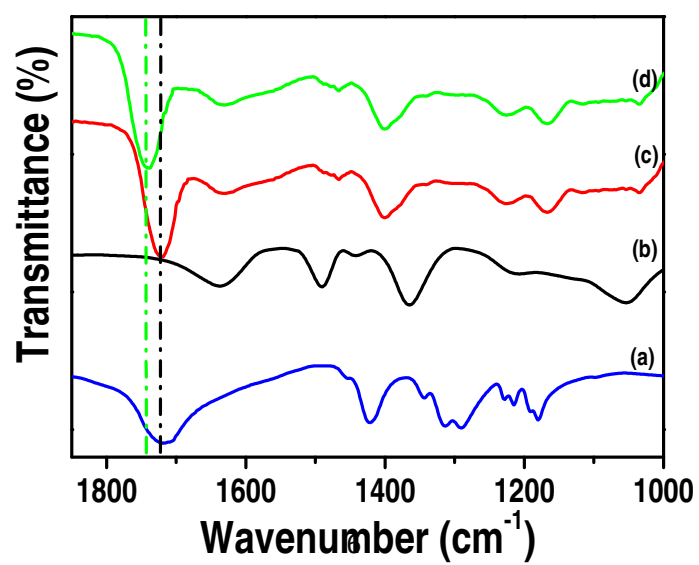


Figure S9. FT-IR spectra of (a) EDTA, (b) GNRs, (c) GNR-EDTA, and (d) GNR-EDTA after addition of 200 ppm Pb(II). The change in spectral feature at 1710 cm^{-1} is marked.

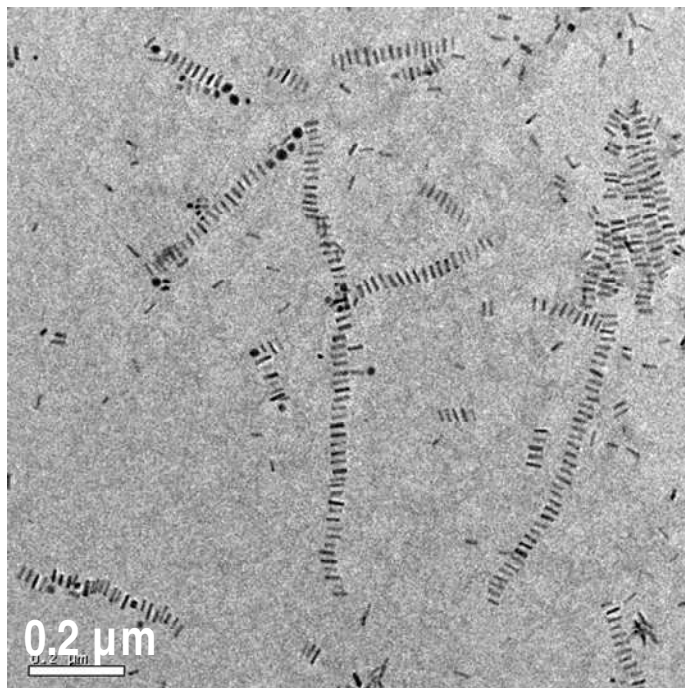


Figure S10. TEM images of ladder-like assemblies formed at pH= 3.5.

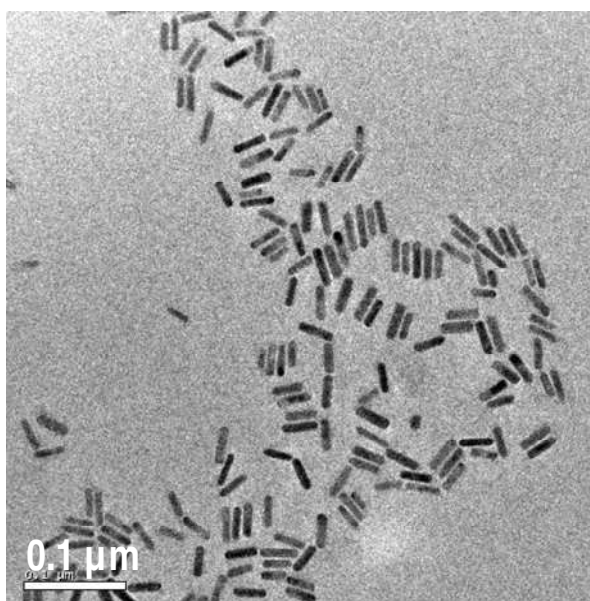


Figure S11. TEM images of randomly arranged GNRs upon addition of EDTA-Pb(II) complex. No assembled structures can be seen.

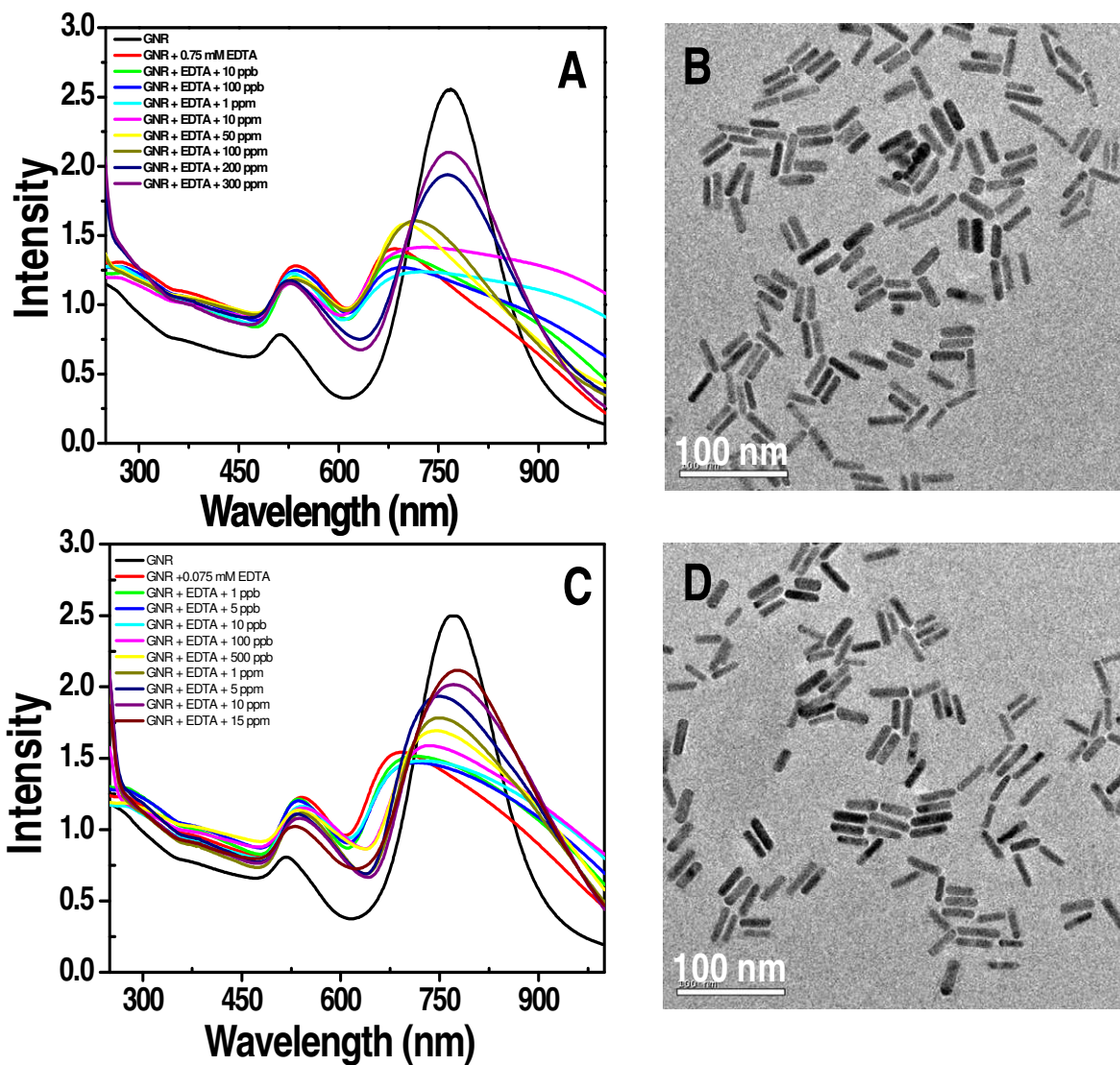


Figure S12. UV/Vis spectra showing the spectral changes happening to the side-by-side assembled GNR-EDTA (0.75 mM) sample upon the addition of A) Fe (II), C) Fe(III) and the corresponding TEM image after the disassembly: B) and D).

Raman band assignment	Raman shift (cm ⁻¹)
ring C-C stretching	1640
ring C-C stretching	1605
ring C-C stretching	1555
+ ring deformation	1490
ring C-C stretching	1460
N-phenyl stretching	1389
ring C-C stretching	1315
ring C-H bend (=)	1195
ring C-H bend (=)	1135
ring skeletal vib. of radical orientation	995
ring skeletal vib. of radical orientation	935
ring C-H bend (\perp)	830
ring C-H bend (\perp)	780
ring C-H bend (\perp)	754
ring skeletal vib. of radical orientation	641
ring skeletal vib. of radical orientation	590
ring skeletal vib. of radical orientation	545
Ph-C+-Ph bend (\perp)	444
Ph-C+-Ph bend (\perp)	368
Breathing of central bonds	246
(=) and (\perp) means in-plane and out-of-plane, respectively	

Table 1. Assignment of Raman bands of the SERS spectrum of CV shown in Figure 8B.

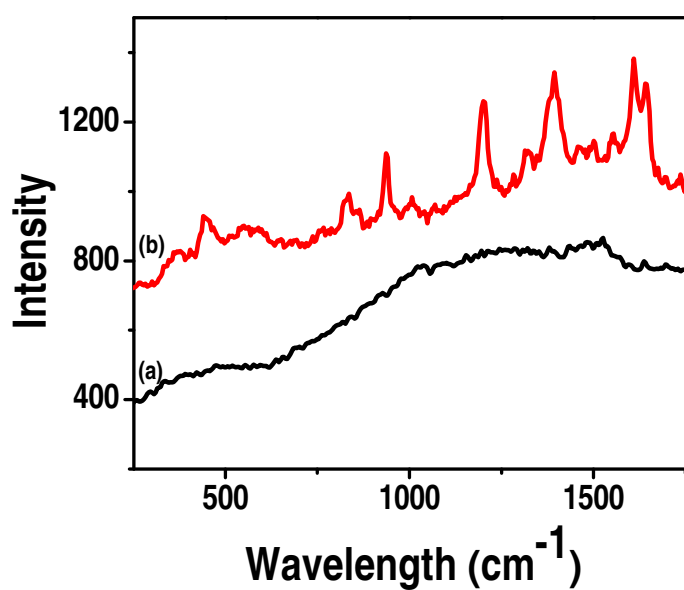


Figure S14. a) Raman spectrum from parent GNRs and b) SERS spectrum collected from GNR assemblies formed from same GNRs.

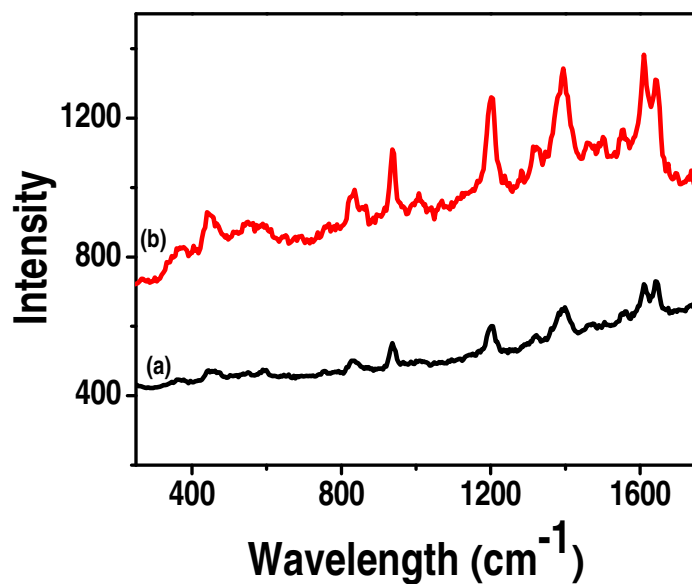


Figure S15. Plot depicting the comparison of SERS activity of aggregated spherical nanoparticles (a) and that of the GNRs assembly (b) under similar conditions.

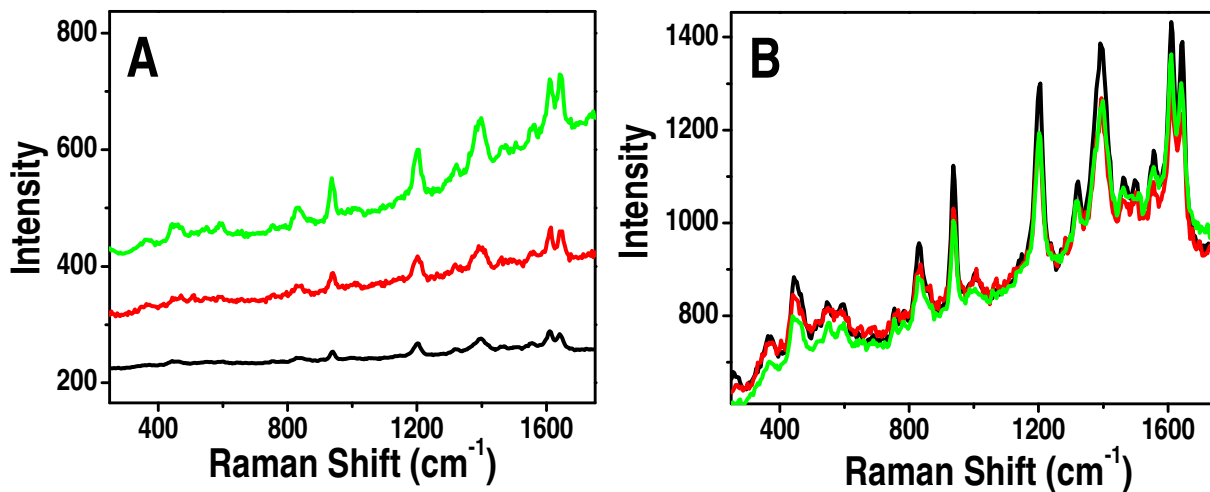


Figure S16. SERS spectra taken from different parts of A) aggregates of spherical nanoparticles and B) GNR assembly. Different colors of the spectra refer to different location from where the spectra are taken.